Earth Reinforcement, Ochiai, Yasufuku & Omine (eds) © 1996 Balkema, Rotterdam. ISBN 905410 833 9

Centrifugal and finite element modelling of reinforced embankments on soft clay

J.S.Sharma & M.D.Bolton
Cambridge University Engineering Department, UK

ABSTRACT: The behaviour of reinforced embankment on soft clay is explored using centrifugal as well as finite element modelling with particular emphasis on the depth of the clay foundation. In the finite element analyses, the stress-induced anisotropic behaviour of the clay foundation was modelled. The experimental and numerical results were found to be in close agreement with each other. Lateral displacements, excess pore pressures and tension in the reinforcement for a deep clay foundation was found to be much more widespread compared to that for a shallow clay foundation for which it was localised underneath the slope of the embankment. The magnitude of maximum tension induced in the reinforcement was found to be only of the order of lateral thrust in the embankment but even such small tension was sufficient to prevent the failure of the embankment.

1 INTRODUCTION

The design of embankments founded on soft clay is primarily influenced by the potential instability during or immediately after the construction of the embankment when the loading on the clay foundation is at its maximum but the shear strength of the clay foundation is greatly reduced due to the generation of excess pore pressures. One of the solutions to this short-term instability problem is to provide a geosynthetic reinforcement at the interface between the embankment and the soft clay foundation. The reinforcement can reduce both the spreading of the embankment and the lateral displacement of the clay foundation by mobilising tensile forces. Although this technique is widely used now-a-days and data is available from several instrumented field trials, the behaviour of reinforced embankments on soft clay is far from clear. This paper describes an investigation into the behaviour of such embankments using the techniques of centrifugal and finite element modelling with particular emphasis on the effectiveness of the reinforcement with respect to the depth of the clay foundation.

2 CENTRIFUGE MODELLING

Centrifuge modelling, because of its ability to reproduce the same stress levels in a small-scale model as in a full-scale prototype, is a powerful tool in exploring soil-structure interaction problems. Furthermore, it also offers the advantage of smaller size, ease of management and control, shorter consolidation time-scale, lower costs and the option to continue the test to failure.

In the present study, three 1:40 scale centrifuge model tests were performed using the Cambridge University 10 m balanced beam centrifuge. Figure 1 shows the details of typical centrifuge models. Table 1 gives a brief description of each of the three centrifuge tests. Due to inherent symmetry about the centre line, only one half of the structure was modelled. Such an arrangement helped in constructing a reasonable sized model within a relatively small strongbox. A special clamp was built to anchor the model reinforcement to the right side of the liner. This clamp, while preventing the horizontal movement of the reinforcement, allowed for its vertical movement following the settlement of the clay foundation.

A smooth nylon sheet was glued to the inside vertical surfaces of the liner in order to reduce the friction between the liner and the soil. The speswhite kaolin clay slurry was consolidated to a maximum vertical pressure of 100 kPa in a consolidometer. Two days before the day of the centrifuge test, it was unloaded and removed from the consolidometer and trimmed to the dimensions of the model. The clay block and the liner were then placed in a strongbox. A matrix of black plastic markers was installed on the front face of the clay block which was used for measuring clay displacements from the photographs taken in-flight through the front perspex window.

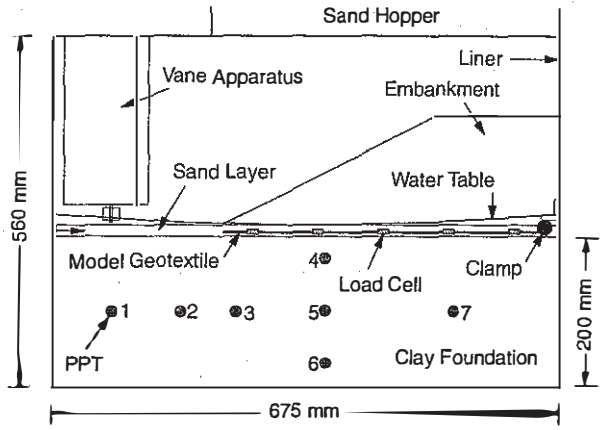

Deep Clay Foundation

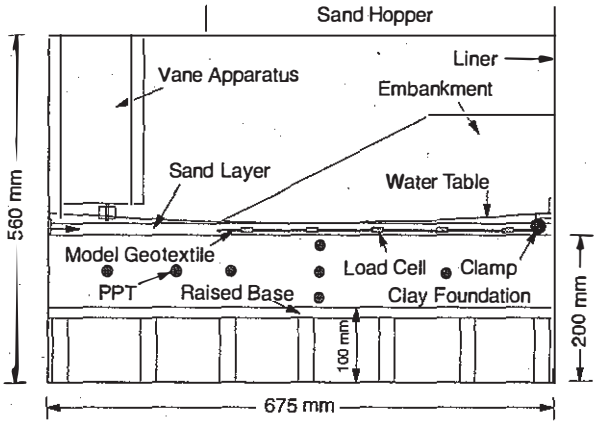

Shallow Clay Foundation

Figure 1 Arrangement of centrifuge models

Table 1 Description of centrifuge tests

Test Code	Depth of Clay (mm)	Type of Reinforcement
JSS7	200	Geotextile
JSS8	200	Unreinforced
JSS12	100	Geotextile

A multifilament woven polyester model geotextile was used as a reinforcement. It was supplied by Akzo Industrial Corporation b.v., The Netherlands. The process of scaling-down the prototype reinforcement to obtain the model reinforcement has been discussed in detail by Springman et al. (1992). At 40 g, the model geotextile represented a prototype geotextile having a tensile strength of 380 kN/m at 10% axial strain. In order to record the tensile force induced in the reinforcement during and after the embankment construction, five load cells were constructed on the model reinforcement. A typical load cell consisted of approximately 12.5 mm wide and 0.7 mm thick strip of epoxy resin cast across the entire width of the reinforcement. The epoxy strip was reinforced using a combination of insulated copper wires and carbon fibre strips. The main objective of reinforcing the epoxy strip was to keep its thickness small so that it would not alter the characteristics of the reinforcement. The details of the load cell have been described by Springman et al. (1992) and the procedure and results of its calibration has been described by Bolton and Sharma (1994).

Before loading the model on to the centrifuge, the model geotextile with calibrated load cells was attached to the clamp and was placed directly on top of the model clay foundation. A 10 mm thick layer of Leighton-Buzzard 25/52 sand was then placed uniformly over the reinforcement. A typical centrifuge test consisted of first bringing the clay foundation to a state of hydrostatic pore pressure equilibrium with water table at 10 mm above the top surface of the clay foundation. In-flight vane shear tests were then carried out at different depths at a site sufficiently away from the site of embankment construction. The undrained shear strength of the clay foundation obtained from these in-flight vane shear tests was 10-14 kPa. An embankment was then placed in-flight in 20 stages (15 sec. time interval between successive stages) by pouring Leighton-Buzzard 25/52 sand from a hopper mounted on the top of the strongbox.

Rapid construction of the embankment caused significant deformation of the clay foundation. Excess pore pressures in the clay foundation and tension in the reinforcement both increased as the embankment construction progressed. The clay foundation for test JSS8 (unreinforced, deep clay foundation) failed when about 85% of the embankment was constructed. No failure was observed for the reinforced cases. However, the lateral displacements for test JSS7 (deep clay foundation) were significantly greater than those for test JSS12 (shallow clay foundation). The magnitude of maximum excess pore pressure in the clay foundation was almost the same for all the centrifuge tests but the distribution of excess pore pressure was much more widespread in the case of deep clay foundation, with excess pore pressures of up to 25 kPa observed in the passive zone away from the toe of the embankment. Maximum tension in the reinforcement was higher for test JSS7 as compared to that for test JSS12. Also, the tension profile plotted along the width of the reinforcement showed a distinct peak below the crest of the embankment for test JSS12 but not for test JSS7 for which it reached a plateau beyond the crest of the embankment.

3 FINITE ELEMENT MODELLING

A selected increment version of the finite element program CRISP mounted on an IBM compatible PC was used for the analyses presented here. CRISP is specified in its User's Manuals Vol. 1 & 3 (Britto & Gunn, 1990). Figure 2 shows the details of the mesh used for the analyses.

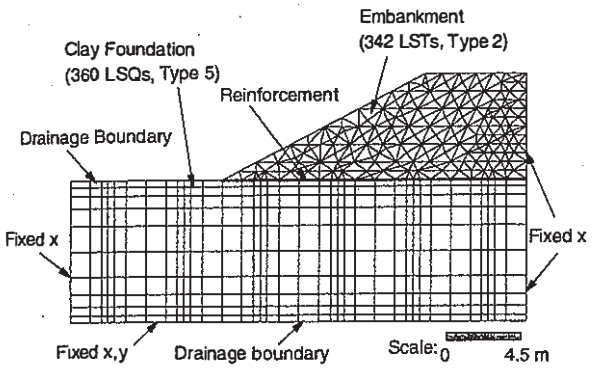

Figure 2 Details of the finite element mesh

It is a two-dimensional plane strain mesh with boundary conditions similar to those of the centrifuge model with all dimensions 40 times those of the centrifuge model, i.e. it represents an idealised prototype. The mesh shown in Figure 2 represents tests with a deep clay foundation. The mesh for test with a shallow clay foundation was obtained by shrinking the part of the mesh representing the clay foundation in the vertical direction. The clay foundation was modelled using linear strain quadrilaterals (LSQs) with displacements and pore pressures unknown, and the embankment was modelled using linear strain triangles (LSTs) with displacements unknown. The in-flight construction of the embankment was simulated by adding the LSTs in six layers. The shape of each of the six layers was derived from in-flight photographic measurements. The reinforcement was modelled using linear elastic bar elements incapable of taking any compression and bending. The soil-reinforcement interfaces were modelled using the 6-noded interface elements with a Mohr-Coulomb type slip criterion.

3.1 *Modelling the clay foundation*

It is generally well-understood that one-dimensionally consolidated clays exhibit stress-induced anisotropy. The undrained shear strength (s_u) of such a clay reduces by as much as 50% as the direction of principal stress changes from nearly vertical in the active zone to nearly horizontal in the passive zone. An anisotropic soil model is necessary if this behaviour is to be modelled accurately. However, the use of anisotropic constitutive models is not very common and all elasto-plastic and elastic-perfectly plastic models in CRISP are isotropic. Nevertheless, it is possible to make use of an isotropic model but with the specification of an average s_u value (usually obtained from direct simple shear tests) when analysing reinforced embankments on soft clay. It has been experimentally observed (e.g. Prevost, 1979) that an s_u value obtained from direct simple shear (DSS) test is approximately equal to the average of s_u values obtained from triaxial compression and extension tests, i.e. the s_u value obtained from DSS test is approximately equal to 75% of that obtained from triaxial compression test.

In the analyses presented here, the clay foundation was modelled using the Schofield model which is essentially a Cam-clay model but with a Hvorslev surface and a tension cut-off surface on the dry side of the Critical State Line (CSL). The choice of the Schofield model was influenced by the fact that the clay foundation was heavily overconsolidated at the top with the overconsolidation ratio ranging from 33 at the surface to around 4 at a depth of 3 m. For the Schofield model, assuming that all other parameters are constant for a given soil, its s_u value depends solely on the maximum isotropic consolidation pressure. In the analyses presented here, the value of the maximum isotropic preconsolidation pressure was reduced from 133 kPa (corresponding to a maximum vertical consolidation pressure of 100 kPa) to 94 kPa in order to obtain average s_u values corresponding to the direct simple shear conditions. Most of the Critical State parameters for kaolin were taken from Al-Tabbaa (1987) and Stewart (1989). Table 2 gives all the parameters specified for the clay foundation.

3.2 *Modelling the sand embankment*

The sand embankment was modelled using the elastic-perfectly plastic model with Mohr-Coulomb yield criterion. A critical state angle of internal friction was used for unreinforced embankment in anticipation of large strains in the later stages of the analyses whereas a higher value of angle of internal friction was used for the reinforced embankment to take into account the increase in strength due to dilation at small strain anticipated throughout the analysis. A better option (not available in CRISP) would have been to use an elastic-perfectly plastic model with non-associated flow rule to represent the sand embankment. A small value of cohesion (c = 1 kPa) was specified for the sand embankment for the purpose of avoiding numerical instabilities near the toe of the embankment. The average bulk unit weight of the sand embankment was reduced from 17.1

kN/m^3 (achieved in centrifuge tests) to 16 kN/m^3 to compensate for the friction between the sand and the inner sides of the strongbox which was estimated using the coefficients of friction obtained in shear box tests (Sharma, 1994). Table 2 gives all the parameters specified for the sand embankment.

3.3 *Modelling the geotextile and its interfaces*

As mentioned above, the geotextile was modelled using linear elastic bar elements. The stiffness of the geotextile was derived from the load-elongation curve obtained by conducting 1%/min tensile tests on 200 mm wide specimens with 200 mm gauge length. Table 2 gives the parameters specified for the reinforcement.

The soil-geotextile interfaces were modelled using 6-noded slip elements. The parameters specified for the two interfaces are given in Table 2. Effective strength parameters were specified because the interfaces are located at the upper drainage boundary. No testing was carried out to obtain these parameters. It is worth mentioning that very low shear stresses were obtained at both the interfaces after carrying out a few preliminary analyses which implies that slip at either of the two interfaces is unlikely and that the interface behaviour is likely to remain largely elastic throughout the analysis. Consequently, the strength parameters of the interfaces are less important than their elastic shear stiffnesses which were taken equal to those of the adjacent soils.

3.4 *Outline of the analyses*

Three analyses were carried out in the present study. Table 3 gives the details of these analyses. For all the analyses, the embankment construction was carried out in six stages (one layer per stage). The total time allowed for embankment construction was 6 days and 3 hours.

Table 3 Details of the finite element analyses

Analysis	Test Code	Details
U8FAST	JSS8	Unreinforced, deep clay foundation.
R8GTX	JSS7	Reinforced , deep clay foundation.
R4GTX	JSS14	Reinforced, shallow clay foundation.

4 COMPARISON OF RESULTS

Figure 3 shows the horizontal displacement of node 163 (located in the mesh representing the clay foundation) as predicted by analysis U8FAST. As mentioned in section 2, the clay foundation for the unreinforced embankment (test JSS8) failed when 85% of the embankment was constructed. It is clear from figure 3 that the approximate treatment of the anisotropic behaviour of the clay foundation has modelled its behaviour fairly accurately.

Table 2 Parameters specified for the finite element analyses

Clay Foundation	Sand Embankment	Geotextile Reinforcement	Soil-Geotextile Interfaces	
			Clay-geotextile	Sand-geotextile
κ = 0.028	E = 4500 to 10000	E_r = 2.3E+6	c = 0.0	c = 0.0
λ = 0.187	ν = 0.3	ν = 0.2	ϕ = 25.8	ϕ = 35
M = 0.755	γ = 16.0	A_r = 0.00212	K_n = 3500	K_n = 13000
Γ = 3.00	c = 1.0		K_s = 1000	K_s = 3800
ν = 0.3	ϕ = 35 or 50		K_{sres} = 10	K_{sres} = 40
γ = 16.3			t = 0.06	t = 0.06
k_h = 1.43E-9				
k_v = 0.50E-9				
H = 0.59				
S = 2.00				

Note: In the above table, κ — slope of the swelling line; λ — slope of the compression line; M — slope of the CSL in q-p' space; Γ — critical state specific volume at p' = 1 kPa; ν — Poisson's ratio; γ — bulk density in kN/m^3; c — cohesion in kPa; ϕ — angle of intemal friction in degrees; E — Young's modulus in kPa; E_r and A_r — Young's modulus in kPa and area of cross-section per unit width in m^2/m for the reinforcement respectively; H — slope of the Hvorslev surface; S — slope of the tension cut-off; k_h and k_v — respectively the horizontal and vertical permeabilities of the clay foundation in m/sec; K_n, K_s and K_{sres} — respectively the normal, shear and residual shear stiffness of the slip element in kPa; and t — thickness of the slip element in m.

It is worth mentioning that for analysis U8FAST, up to 30% deviatoric strains were observed in the embankment at the instant when it failed, thus justifying the use of Critical State angle of internal friction for the sand.

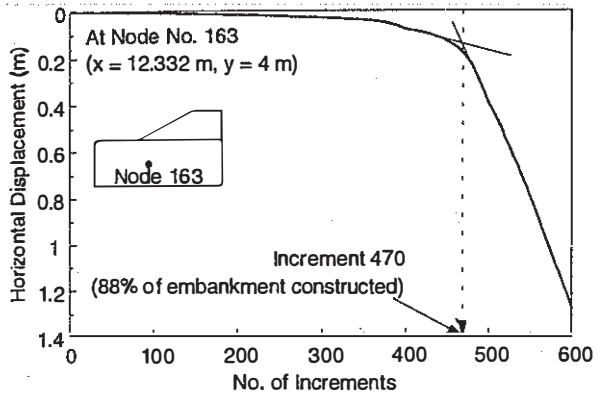

Figure 3 Lateral displacement of the clay foundation (analysis U8FAST)

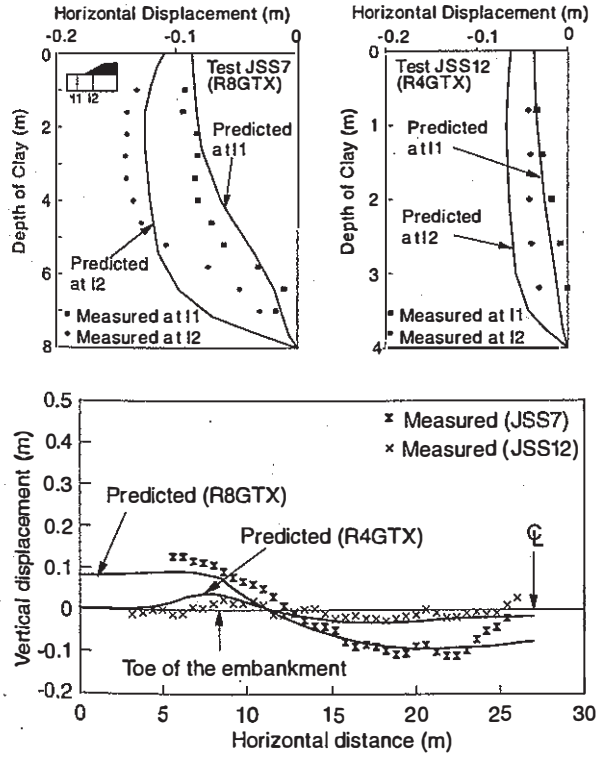

Figure 4 Displacement of the clay foundation

The horizontal and vertical displacements of the clay foundation were reasonably well-predicted by the analyses as seen from figure 4 which shows a comparison of horizontal displacement at two "inclinometer" locations (each consisting of a column of black plastic markers in the case of centrifuge tests and a column of nodes in the case of finite element analyses) and vertical displacements at a level 1m below the top surface of the clay foundation. As observed in centrifuge tests, the magnitude of lateral displacement was much less for shallow clay foundation compared to the lateral displacement for the deep clay foundation.

Excess pore pressures in the clay foundation were also reasonably well-predicted as seen from figure 5 and Table 4 which compare the measured and predicted excess pore pressures at various locations (shown in figure 1). The distribution of excess pore pressures was much more widespread for the deep clay foundation as compared to the shallow clay foundation for which it was localised underneath the shoulder of the embankment. Slight underprediction of excess pore pressures underneath the crest of the embankment (PPT Nos. 5, 6 & 7) for deep clay foundation may be attributed to the fact that a constant value of permeability was specified in the analyses which may have resulted in the prediction of a higher degree of consolidation during the embankment construction. A better option (not available in CRISP) would have been to model the permeability of the clay foundation as a function of its current void ratio.

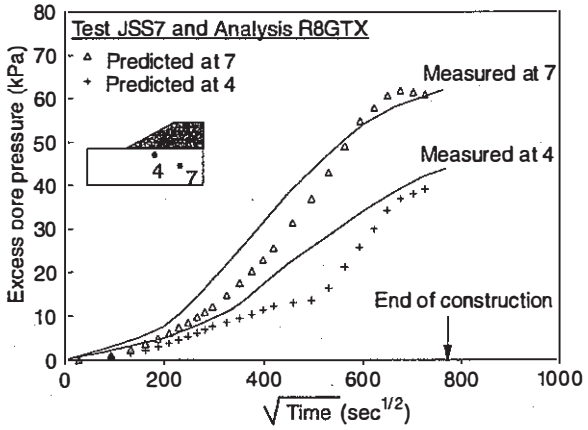

Figure 5 Excess pore pressure in the clay foundation during embankment construction

Table 4 Excess pore pressures in the clay foundation just after embankment construction

PPT No. →	1	2	3	4	5	6	7
JSS8	33	24	29	42	—	70	—
U8FAST	13	20	27	32	40	55	47
JSS7	—	24	33	45	49	64	65
R8GTX	10	19	25	43	38	54	55
JSS12	2	7	18	44	44	34	77
R4GTX	4	5	14	37	39	39	77

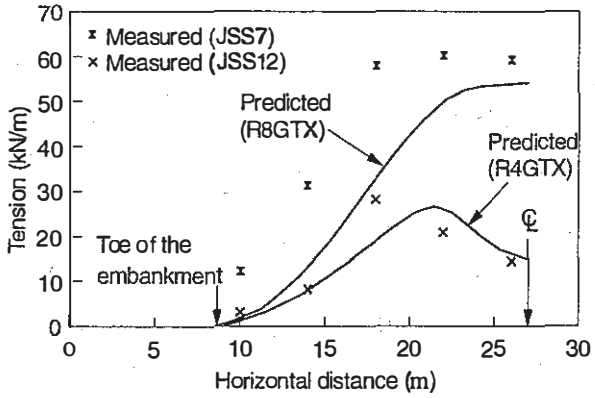

Figure 6 Tension induced in the reinforcement

Figure 6 shows the measured and predicted tension profiles for the reinforced case. As seen from figure 6, the tension profile was well-predicted for the shallow clay foundation. For the deep clay foundation, the maximum tension in the reinforcement was well-predicted but the tension underneath the slope of the embankment was underpredicted. As observed in the centrifuge tests, the magnitude of maximum tension in the reinforcement was much less for the shallow clay foundation as compared to the deep clay foundation. For the deep clay foundation, maximum tension in the reinforcement was only of the order of the lateral thrust in the embankment. This is consistent with the observation of low tension levels in the reinforcement from several field trials. However, even such a low level of tension was sufficient to prevent the failure of the clay foundation.

5 CONCLUSIONS

The behaviour of reinforced embankments on soft clay has been explored using centrifugal as well as finite element modelling. A new type of load cell was successfully used in recording the tension induced in the reinforcement during the embankment construction. In the finite element analyses, the stress-induced anisotropic behaviour of a one-dimensionally consolidated clay foundation was modelled using an approximate approach. The success of using such an approach is clear from reasonably good predictions of the collapse height of an unreinforced embankment, displacement and excess pore pressures in the clay foundation and the tension in the reinforcement. Maximum tension induced in the reinforcement was found to be only of the order of the lateral thrust in the embankment but it was sufficient to prevent the failure of the deep clay foundation. The lateral displacement, excess pore pressures and tension in the reinforcement were found to be localised underneath the crest of the embankment founded on a shallow clay foundation.

ACKNOWLEDGEMENTS

The experimental part of the work described in this paper was funded by the Transport Research Laboratory, UK. The help and technical support of the staff of Geotechnical Centrifuge Centre and Soil Mechanics Laboratory of Cambridge University is gratefully acknowledged. The authors wish to thank Dr. Arul Britto for his help in the finite element modelling. The first author is grateful for the financial support provided by the Nehru Trust for Cambridge University and ORS award given by the CVCP of British University.

REFERENCES

Al-Tabbaa, A. (1987). Permeability and stress-strain response of speswhite kaolin. Ph.D. thesis. Cambridge University, UK.

Bolton, M.D. and Sharma, J.S. (1994). Embankments with base reinforcement on soft clay. Proc. Centrifuge'94, pp 587-592.

Britto, A.M. and Gunn, M.J. (1990). CRISP90 - User's and Programmer's Guide, Vols. 1 & 3, Cambridge University Engg. Department, UK.

Prevost, J.H. (1979). Undrained shear tests on clays. Journal of Geotechnical Engineering Division, ASCE, Vol. 105, No. 1, pp 49-64.

Sharma, J.S. (1994). Behaviour of reinforced embankments on soft clay. Ph.D. thesis, Cambridge University, UK.

Springman, S.M., Bolton, M.D., Sharma, J. and Balachandran, S. (1992). Modelling and instrumentation of a geotextile in a geotechnical centrifuge. Proc. IS Kyushu'92, Japan, pp 167-172.

Stewart, D.I. (1989). Groundwater effects on in-situ walls in stiff clays. Ph.D. thesis, Cambridge University, UK.